

Rotary Ultrasonic Motors Actuated By Traveling Flexural Waves

Yoseph Bar-Cohen^a, Xiaoqi Bao^a, and Willem Grandia^b,

^aJet Propulsion Laboratory, Caltech, Pasadena, CA 91109, yosi@jpl.nasa.gov

^bQuality Material Inspection (QMI), Costa Mesa, CA 92627

ABSTRACT

Efficient miniature actuators that are compact and consume low power are needed to drive telerobotic devices and space mechanisms in future NASA missions. Ultrasonic rotary motors have the potential to meet this NASA need and they are developed as actuators for miniature telerobotic applications. The technology that has emerged in commercial products requires rigorous analytical tools for effective design of such motors. A finite element analytical model was developed to examine the excitation of flexural plate wave traveling in a rotary piezoelectrically actuated motor. The model uses annular finite elements that are applied to predict the excitation frequency and modal response of an annular stator. This model is being developed to enable the design of efficient ultrasonic motors (USMs) and it incorporates the details of the stator which include the teeth, piezoelectric crystals, stator geometry, etc. The theoretical predictions were corroborated experimentally for the stator. Parallel to this effort, USMs are made and incorporated into a robotic arm and their capability to operate at the environment of Mars is being studied. Motors with two different actuators layout were tested at cryovac conditions and were shown to operate down to -150°C and 16-mTorr when the activation starts at ambient conditions.

Keywords: Piezoelectric Motors, Ultrasonic Motors (USMs), Stators and Rotors, Modal Analysis, Actuators, Active Materials,

1. INTRODUCTION

Actuators are used to operate NASA telerobotic devices that include robotic arms, rovers, etc., as well as space mechanism/instruments such as release mechanisms, antenna and instrument deployment, positioning devices, aperture opening and closing devices, etc. Increasingly, actuators need to have reduced size, mass, and power consumption, as well as lower cost to NASA. These constraints are necessary to allow meeting mission requirements with as many experiments and tasks as possible while conforming to strict mass, size, power, and cost allocations. This trend is straining the specifications of actuation and articulation mechanisms that drive space and planetary instruments. The miniaturization of conventional electromagnetic motors is limited by practical manufacturing difficulties. These types of motors are compromising speed for torque using speed-reducing gears. The use of gear adds mass, volume and complexity as well as decreases the motor drive system reliability due the involvement of a larger number of system components. The recent introduction of rotary ultrasonic motors (USMs) enabled a new avenue of effective actuation technology for drive mechanisms of miniature instruments [1-5]. These motors have high torque density at low speed, high holding torque, simple construction, can be made in annular shape (for optical application, electronic packaging and wiring through the center), and have a quick response. JPL is developing these motors for operation at such planetary environments as Mars over an extended period, where the temperature is as low as -120°C and the ambient pressure is about 6-torr. This range of temperatures and pressures is beyond the specifications of commercial piezoelectric motors even though there is no technical reason why these motors would not work. Efforts are made to understand the drive mechanism of USMs and develop alternative stator drive approaches to enhance the efficiency, longevity and operability of these motors. A theoretical model was developed to allow predicting the response of the stator to various drive frequencies and the results were corroborated experimentally.

Generally, ultrasonic motors [5] can be classified by their mode of operation (static or resonant), type of motion (rotary or linear) and shape of implementation (beam, rod, disk, etc.). Despite the distinctions, the fundamental principles of solid-state actuation tie them together: microscopic material deformations (usually associated with piezoelectric materials) are amplified through either quasi-static mechanical or dynamic/resonant means. Several of the

motor classes have seen commercial application in areas needing compact, efficient, and intermittent motion. Such applications include: camera auto focus lenses, watch motors and compact paper handling. Obtaining the levels of torque-speed characteristics of USMs using conventional motors requires adding a gear system to reduce the speed, thus increasing the size, mass and complexity of the drive mechanism. USMs are fundamentally designed to have a high holding force, providing effectively zero backlash. Further, since these motors are driven by friction the torque that would cause them to be backdriven at zero power is significantly higher than the stall torque. The number of components needed to construct ultrasonic motor is small minimizing the number of potential failure points. The general characteristic of USMs makes them attractive for robotic applications where small, intermittent motions are required.

In Figure 1 the principle of operation of an ultrasonic motor (flexural traveling wave ring-type motor) is shown as an example. A traveling wave is established over the stator surface, which behaves as an elastic ring, and produces elliptical motion at the interface with the rotor. This elliptical motion of the contact surface propels the rotor and the drive-shaft connected to it. Teeth on the top section of the stator are intended to form a moment arm to amplify the speed. The operation of USM depends on friction at the interface between the moving rotor and stator, which is a key issue in the design of this interface for extended lifetime.

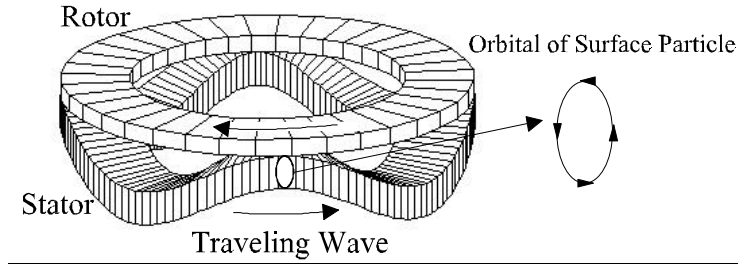


Figure 1. Principle of Operation of a Rotary Traveling Wave Motor.

2. PRINCIPLE OF OPERATION

Ultrasonic motors are driven by a mechanism that generates gross motion through the amplification and repetition of micro-deformations of active materials. Active materials are employed to induce orbital motion on the surface of a stator at the contact points with a rotor. A frictional interface between the rotor and stator rectifies the micro-motion to produce macro-motion of the rotor. This mechanism is illustrated in Figure 1. The active material, which is a piezoelectric material excites a traveling flexural wave within the stator leading to elliptical motion of the surface particles. Teeth are used to enhance the speed that is associated with a propelling effect of the surface particles. The rectification of the micro-motion at the interface is obtained by pressing the rotor on top of the stator and the frictional force between the two causes the rotor to spin. This motion transfer operates as a gear and it leads to a much lower rotation speed than the wave frequency and it can be a factor of several thousands.

A stator substrate is assumed to have a thickness, t_s , with a set of piezoelectric crystals that are bonded to the back surface of the stator in a given pattern of poling sequence and location. The thickness of the piezoelectric crystals is t_p . The total height, h , is the sum of the thickness of the crystals and the stators (bonding layer is neglected). The overall height of the stator is also allowed to vary with radial position. The outer radius of the disk is b and its inner radius (the hole radius) is a . To generate traveling wave, the poling direction of the piezoelectric crystals is structured such that a quarter wavelength out-of-phase is formed. This poling pattern is also intended to eliminate extension in the stator and maximize bending. The teeth on the stator are arranged in a ring at the radial position.

To generate a traveling wave within the stator two orthogonal modes are activated simultaneously. These modes are induced by a stator that is constructed with the drive piezoelectric actuators in the form of two sections of poling pattern that are bonded to the stator. Geometrical examination of this pattern shows that driving the two sections using $\cos(\omega t)$ and

$\sin(\omega t)$ signals, respectively, will produce a traveling wave with a frequency of $\omega/2\pi$. Also, by changing the sign on one of the drive signals, the traveling wave would reverse its direction.

3. THEORETICAL MODELING

The equation of motion of the ultrasonic motor can be derived from the Hamilton's principle. The analytical model has been derived by many authors (e.g. Hagood and A. McFarland [5], Kagawa et al [6]). The generalized equation of motion of the stator can be summarized as

$$\begin{aligned} [M]\{\ddot{x}\} + [C]\{\dot{x}\} + [K]\{x\} &= [P]\{j\} + \{F_N\} + \{F_T\} \\ [P]^T\{x\} - [G]\{j\} &= \{Q\} \end{aligned}$$

where $[M]$, $[C]$, $[K]$, $[P]$, $[G]$, are the mass, damping, stiffness, electromechanical coupling, and capacitance matrices, respectively. The vectors $\{\xi\}$, $\{\phi\}$, $\{F_N\}$, $\{F_T\}$, and $\{Q\}$ are the modal amplitude, the electric potential vectors the normal external force, the tangential external force and the charge vectors, respectively.

The modal amplitude $\{\xi\}$ and other generalized coordinates can be defined through energy methods such as Rayleigh Ritz method [5]. However, this method smears the contribution of the teeth and the variation of the stator ring as well as the support disk along the radial direction and may lead to undesirable results. Even though, 3-D finite element method (FEM) was reported [6] to be used to accurately predict the modal frequencies and transient response of the stator, it is computational intensive process. Further, the calculated response modes and associated frequencies that are determined by the 3-D FEM needs to be identified visually to find the designed mode. Due to the disadvantages for the methods mentioned above the modified annular finite element described in [7] is used and it is based on the symmetrical characteristics of the ultrasonic motors. The annular finite element is shown as in Figure 2, where w_1 , w_2 , ψ_1 , and ψ_2 are the degree of freedoms. The transverse displacement w across each element is assumed to be of the form given by the equation

$$w(r, \theta, t) = (a_0 + a_1 r + a_2 r^2 + a_3 r^3) \cos m\theta \cos(\omega_n^m t), \text{ for } R_1 < r < R_2$$

where ω_n^m is the radial resonance frequency and the index m , n are mode along the θ and r direction, respectively. If we assume that the transverse shear and rotary inertial effects are negligible, the elemental mass, stiffness can be derived using the standard variational methods. Thus, the natural frequency and modal shape can be found by solving the eigenvalue problem.

$$\{[K] - (\omega_n^m)^2 [M]\}\{x_n^m\} = \{0\}$$

Using consistent mass formulations, the effect of the stator teeth can also be included. Details of the formulation of other generalized coordinates are treated similar to those in [7] and will be presented by the authors' in a future publication.

4. ANALYSIS OF PIEZOELECTRIC MOTORS

The analysis of the nonlinear, coupled rotor-stator dynamic model discussed above allows predicting the stator steady state and transient response as a function of critical design parameters such as interface normal force, tooth height, stator radial cross section and piezoelectric wafers thickness. A finite elements algorithm was incorporated into the analysis and a MATLAB code was developed to determine the modal characteristics of the stator that is actuated by a ring shape series of piezoelectric wafers. The model accounts for the shape of the stator, the piezoelectric poling pattern, the piezoceramic wafers thickness, and the teeth parameters. Once the details of the stators are selected the modal response is determined and is presented on the computer monitor [8] where the various modes are determined. An electronic speckle

pattern interferometry was used to corroborate the predicted modal response and the agreement seems has been very good. Also, using MATLAB an animation tool was developed to view the operation of USMs on the computer display. This tool allows to show the rotation of the rotor while a flexural wave is traveling on the stator (Figure 3).

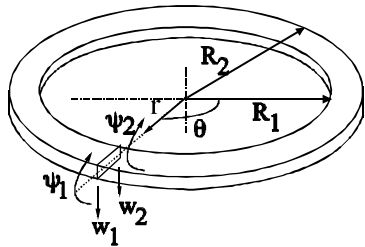


Figure 2: An annular finite element

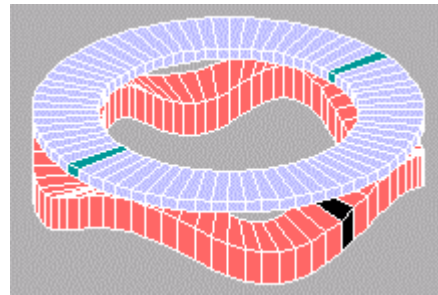
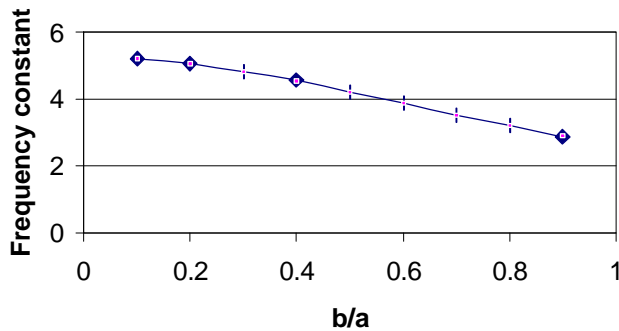


Figure 3: Animation tool for viewing the operation of USM. The stator is shown with traveling wave and the rotor is rotating above the stator.

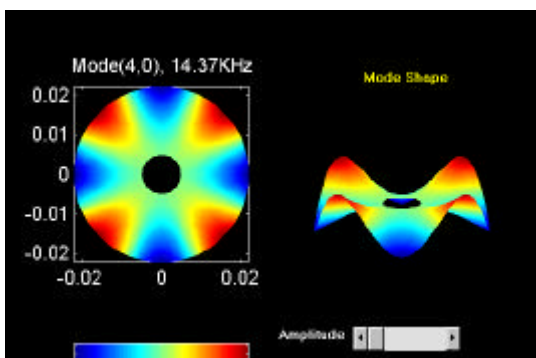
To corroborate the accuracy of the FEM model, we initially examined the case of a simple free-free ring condition. In Figure 4, the Mode (2,0) predictions are confirmed for a case of a ring plate with inner radius b and external radius a , assuming free boundaries on both edges. The frequency constants were determined for the free-free ring and a comparison is shown in Figure 4 between the FEM calculations and the analytically determined data. The small percentage difference between the two is showing a remarkable agreement.



b/a	Analytical	FEM	Difference %
0.1	5.203	5.200	-0.030
0.2	5.053	5.050	-0.015
0.3	4.822	4.821	-0.003
0.4	4.567	4.533	-0.085
0.5	4.203	4.207	0.008
0.6	3.865	3.865	0.000
0.7	3.519	3.523	0.006
0.8	3.200	3.197	-0.004
0.9	2.890	2.894	0.004

Figure 4: Analytical and FEM computations of a free-free annual ring frequency constant and the frequency constant of a free-free annual ring (line and black rhombus - analytical results and white squares - FEM results).

This model that was confirm for the free-free ring case, was extended to the case of a USM stator with double layer of metal plate (stator) having teeth on one side and bonded to a piezoelectric ring on the other side. A schematic cross-section view of the stator for which the model was calculated is shown in Figure 5 (right-bottom). The mode (4,0) characteristic of the stator with teeth and piezoelectric ring is shown in Figure 5 (left). The comparison of the theoretical and experimental results for the resonance frequencies of modes (4,0) and (5,0) is tabulated in Figure 5 (right-top) and it demonstrates the accuracy of the model. Currently, efforts are directed towards accounting for the effect of the rotor and later the effect of the frictional interface will be incorporated.



Mode number	(4,0)	(5,0)
Experimental (KHz)	14.40	22.60
FEM results (KHz)	14.37	23.07

Departure	-0.21%	1.02%
-----------	--------	-------

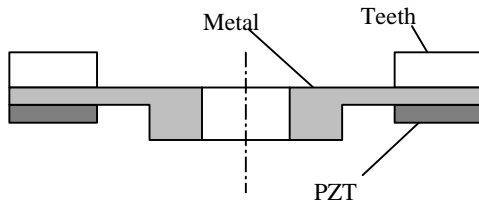


Figure 5: Right Bottom - A cross section view of a USM stator configured with metal disk, PZT ring and teeth; Right-Top-right - A table showing a comparison of the analytical and experimental frequencies of flexural vibration modes for a JPL/QMI experimental stator.; Left - Amplitude view of the flexural vibration mode (4,0) for a JPL/QMI stator.

4. CRYOVAC TESTS OF PIEZOELECTRIC MOTORS

The ability of ultrasonic motor to operate at cryogenic temperatures and vacuum is an important characteristics for planetary applications, such as the planet Mars. To establish a baseline for the performance of a USM that was made by JPL/QMI, a commercial motor with a diameter of 1.2-inch was used (Shinsei Model USR30) and was tested at 150°C and 16 mTorr till failure. At the initial phase of the study no efforts were made to deal with the issue of cold start, where the motor is activated after being brought to the cryovac conditions and held to reach steady state before activation. The USR30 motor failed after over 67 hours of operation at the cryovac conditions. To examine the cause of failure, an ultrasonic C-scan nondestructive test was made and the discontinuities were imaged on the computer monitor as shown in Figure 6. As anticipated, the bond between the stator and piezoelectric ring wafer failed. The use of a continuous ring is subjected to thermal stresses that are aggravated by the cyclic mechanical loading of the motor operation leading to fatigue failure of the bond line. JPL is cooperation with QMI replaced the continuous ring with a segmented and reversed piezoelectric drive (SRPD) wafers allowing to effectively relief the thermal and dynamic stresses at the bonding layer. An SRPD type USM (made by JPL/QMI) failed after 336 hours total of cryovac test (65 hour at -80°C and 25-mTorr plus 271 hours at -150°C and 16-mTorr). A slower operation was observed after about 210 hours, which may have been the result of a single segment failure. After about 8 hours from the beginning, the SRPD motor had an electric wiring disconnect probably due to fatigue, which was fixed. To determine the robustness of the motor during the cryovac test, it was subjected to 36 stall-torque tests. This test result showed that the use of segmented wafer led to more than 5 times longer lifetime operation at low temperature and vacuum environment. While more motors need to be tested to obtain sufficient statistics however the significant difference of 5 times longer longevity is a very encouraging feasibility demonstration. The torque-speed curve for the JPL/QMI is shown in Figure 7. The loop appearance of the curve is the result of the loading and unloading of the motor and the difference between the two is caused by variations in the motor braking mechanism that is used. Preliminary test of the cold start response of the motor showed that there is a need to control the resonance frequency and drive voltage and so far we were able to activate a motor at 70°C of cold start. Other issues that are currently being studied include the performance at cyclic temperature environment and vacuum as on Mars.

5. CONCLUSIONS

A finite element model was developed to analyze the spectral response of the stator of ultrasonic motors. The model account for the piezoelectric wafers layer, the complex geometrical configuration and construction materials. The modal response and the predicted resonance conditions were corroborated experimentally. Further, a user interface interactive tool was developed for operation over a MATLAB platform simplifying the analysis of the modal behavior of USMs and allowing the study of their response to various stator parameters. In addition, cryovac tests were made on USMs and showed that the motors can be driven from room temperature down to -150 ° C and 16-mTorr and still operate for at least several hundred hours. Efforts are currently being made to investigate the issue of cold start for such motors at low temperatures.

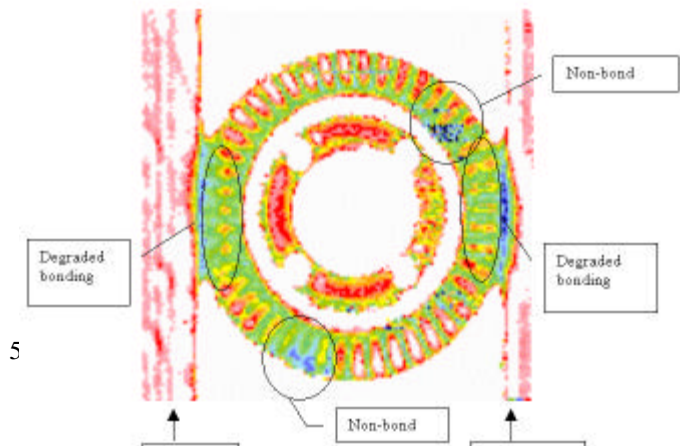
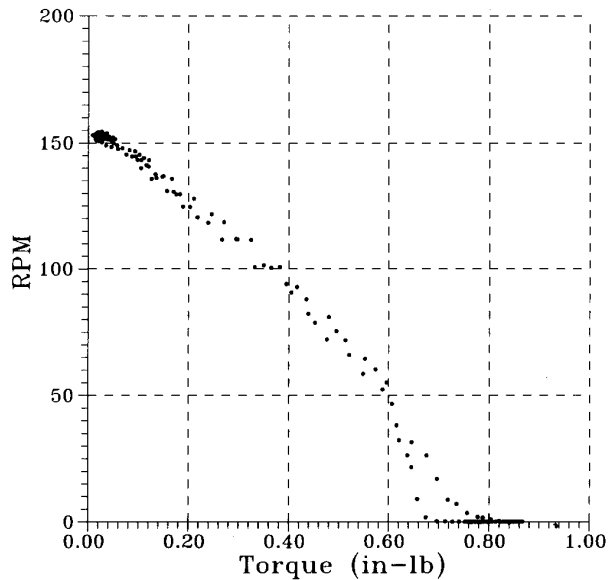


Figure 6: An Ultrasonic C-Scan image of a 1.2" diameter stator (Shinsei) that was subjected to 150°C and 16 mTorr for over 67-h.

Figure 7: Torque-speed performance of a JPL/QMI USM subjected to 150°C and 16 mTorr



ACKNOWLEDGMENT

The results reported in this manuscript were obtained under the Planetary Dexterous Manipulator (PDM) Task, which is currently managed by Dr. Hari Das and up till October 1997 by Dr. Paul Schenker. PDM is a NASA Telerobotics task supported by a JPL, Caltech, contract with NASA Headquarters, Code S, Mr. David Lavery and Dr. Chuck Weisbin are the Managers of TRIWG.

REFERENCES

1. M. Hollerbach, I. W. Hunter and J. Ballantyne, "A Comparative Analysis of Actuator Technologies for Robotics." In *Robotics Review 2*, MIT Press, Edited by Khatib, Craig and Lozano-Perez (1991).
2. A. M. Flynn, et al "Piezoelectric Micromotors for Microrobots" *J. of MEMS*, Vol. 1, No. 1, (1992), pp. 44-51.
3. E. Inaba, et al, "Piezoelectric Ultrasonic Motor," *Proceedings of the IEEE Ultrasonics 1987 Symposium*, pp. 747-756, (1987).
4. J. Wallashek, "Piezoelectric Motors," *J. of Intelligent Materials Systems and Structures*, Vol. 6, (Jan. 1995), pp. 71-83.
5. N. W. Hagood and A. McFarland, "Modeling of a Piezoelectric Rotary Ultrasonic Motor," *IEEE Transactions on Ultrasonics, Ferroelectrics and Frequency Control*, Vol. 42, No. 2, 1995 pp. 210-224.
6. K. Kagawa, T. Tsuchiya and T. Kataoka, "Finite Element Simulation of Dynamic Responses of Piezoelectric Actuators," *J. of Sound and Vibrations*, Vol. 89 (4), 1996, pp. 519-538.
7. D. G. Gorman, "Natural Frequencies of Transverse Vibration of Polar Orthotropic Variable Thickness Annular Plates," *J. of Sound and Vibrations*, Vol. 86 (1), 1983, pp. 47-60.

8. S.-S. Lih, Y. Bar-Cohen and W. Grandia, "Rotary Piezoelectric Motors Actuated By Traveling Waves," Proceedings of SPIE, Vol. SPIE 3041, Smart Structures And Materials 1997 Symposium, Enabling Technologies: Smart Structures and Integrated Systems, Marc E. Regelbrugge (Ed.), ISBN 0-8194-2454-4, SPIE, Bellingham, WA (June 1997), p. 912-917.